Published in final edited form as:
Biochemistry. 2008 September 16; 47(37): 9728–9737. doi:10.1021/bi8006753.

Thioredoxin reductase from *Thermoplasma acidophilum*: a new twist on redox regulation[†,‡]

Hector H. Hernandez[§], **Orlando A. Jaquez**[‖], **Michael J. Hamill**[⊥], **Sean J. Elliott**[⊥], and **Catherine L. Drennan**[§,‖,*]

[§]Department of Chemistry, Massachusetts Institute of Technology, 16-573, 77 Massachusetts Avenue, Cambridge, MA 02139

[‖]Department of Biology, Massachusetts Institute of Technology, 16-573, 77 Massachusetts Avenue, Cambridge, MA 02139

[⊥]Department of Chemistry, Boston University, 590 Commonwealth Avenue, Boston, MA 02215

Abstract

Thioredoxin reductases (TrxRs) regulate the intracellular redox environment by using NADPH to provide reducing equivalents for thioredoxins (Trxs). Here we present the cloning and biochemical characterization of a putative TrxR (Ta0984) and a putative Trx (Ta0866) from *Thermoplasma acidophilum*. Our data identifies Ta0866 as a Trx through its capacity to reduce insulin, and be reduced by *E. coli* TrxR in a NADPH dependent manner. Our data also establish Ta0984 as a TrxR due to its ability to reduce *T. acidophilum* Trx (*ta*Trx), although not in a NADPH or NADH dependent manner. To explore the apparent inability of *ta*TrxR to use NADPH or NADH as a reductant, we carried out a complete electrochemical characterization, which suggests that redox potential is not the source of this non-reactivity (accompanying paper). Turning to crystallographic analysis, a 2.35 Å resolution structure of *ta*TrxR, also presented here, shows that despite the overall structural similarity to the well-characterized TrxR from *E. coli* (R.M.S.D. 1.30 $Å^2$ for chain A), the "NADPH binding pocket" is not conserved. *E. coli* TrxR residues implicated in NADPH binding, H175, R176, R177, and R181 have been substituted with E185, M186, Y187, and M191 in the *ta* protein. Thus, we have identified a Trx and TrxR protein system from *T. acidophilum* for which the TrxR shares overall structural and redox properties with other TrxRs, but lacks the appropriate binding motif to use the standard NADPH reductant. Our discovery of a TrxR that does not use NADPH provides a new twist in redox regulation.

Tight regulation of the cellular redox environment is crucial for cell survival. Cellular viability relies on the reduction of metabolites for energy production, on the oxidation of small molecules to assemble structural scaffolds, and on the maintenance of the proper disulfide state in the extracellular or intracellular environments. An imbalance in redox regulation can trigger

[†]This work was supported by the NIGMS Ruth L. Kirschstein pre-doctoral fellowship GM73569 (H.H.H.), the National Institutes of Health Grant GM65337 (C.L.D.), and the Richard Allan Barry Fund of the Boston Foundation (S.J.E).

[‡]The atomic coordinates and structure factor amplitudes have been deposited in the Protein Data Bank (www.rcsb.org) as entry 3CTY.

[*]To whom correspondence should be addressed at the Massachusetts Institute of Technology, 77 Massachusetts Avenue, Room 16-573, Cambridge, MA 02139. Phone: (617) 253-5622, Fax: (617) 258-7847, cdrennan@mit.edu.

SUPPORTING INFORMATION AVAILABLE

Supporting information contains sequence alignments of TrxRs and Trxs, sequences of *ta*TrxR and *ta*Trx, a figure showing gel analysis of purified protein, figures showing the temperature dependent degradation of NADH and NADPH, results of insulin assays, results of *ta*Trx and *ec*TrxR reduction of DTNB, a figure of FAD in composite omit map density, schematic representation interactions between FAD and *ta*TrxR, and structural comparison figures. This material is available free of charge via the Internet at http//:pubs.acs.org.

a cascade of genetic responses, the most extreme of which can lead to cell death (Reviewed in (1-4).

The principal protein systems that act as reductants are NADPH-dependent thioredoxin reductase (TrxR) / thioredoxin (Trx), and glutathione reductase (GSSGR) / glutathione (GDH) / glutaredoxin (Grx) (Figure 1A) (1, 2, 4-6). NADPH reduces the FAD of TrxRs, which in turn reduces Trs through disulfide exchange (Figure 1B). The TrxR / Trx system is responsible for providing reducing equivalents for many cellular processes including the reduction of ribonucleotide reductase (RNR) during the conversion of nucleotides to deoxynucleotides (7). This reaction is essential for maintaining the appropriate levels of deoxynucleotides in the cell for DNA repair, and for cellular replication (8, 9). The significance of the redox regulation of these and other biochemical pathways has lead to renewed interest in anti-bacterial or anti-tumorgenic therapies that are targeted to disrupt redox regulation (1, 10-13).

Here we study putative TrxR and Trx from *Thermoplasma acidophilum*, an organism first isolated from a self-heating coal refuse pile at the Friar Tuck mine in southwest Indiana. This organism lacks a cell wall and optimal growth occurs at 59 °C and at pH 1-2 (14). Despite the organism's ability to grow at low pH, the cytoplasmic pH of *T. acidophilum* was reported to be between 5.5 and 6.9 (15,16). The 1.56 Mb genomic sequence of *T. acidophilum* encoding 1,509 open reading frames (ORFs) has been reported (17), allowing us to identify a putative TrxR (Ta0984) and Trx (Ta0866).

We report the cloning, expression, and purification of gene products Ta0984 and Ta0866, and show that Ta0866 exhibits thioredoxin-like activity, and that Ta0984 is able to reduce *T. acidophilum* Trx (*ta*Trx), establishing its identity as a thioredoxin reductase. An accompanying paper describes the full electrochemical characterization of *T. acidophilum* TrxR (*ta*TrxR). While the redox potential is within the expected range for TrxRs, we find that the standard TrxR reducing agents NADPH or NADH do not reduce the *ta*TrxR flavin. The X-ray structure of *ta*TrxR to 2.35 Å resolution presented here reveals a major modification of the classic TrxR NADPH binding site, suggesting that *T. acidophilum* may utilize a novel reductant.

EXPERIMENTAL PROCEDURES

Materials

The organism *Thermoplasma acidophilum* (ATCC number 27656) was obtained from the American Tissue Culture Center. TOPO and TOPO Zero Blunt PCR cloning kits were obtained from Invitrogen (Carlsbad, CA). NovaBlue competent cells, Rosetta™ (DE3) pLysS competent cells, and pET28a plasmid were purchased from Novagen (Madison, WI, USA). *pfu*Turbo DNA polymerase and a PCR Optimization Kit were obtained from Stratagene (Cedar Creek, TX, USA). Primers were obtained from Integrated DNA Technologies (Coralville, IA, USA). Nickel nitrilotriacetic acid (Ni-NTA) was purchased from Qiagen (Valencia, CA, USA). Restriction enzymes were purchased from New England BioLabs (Beverly, MA, USA). Kanamycin, chloroamphenicol, TRIS-HCl, ethylenediaminetetraacetic acid (EDTA), and phenylmethylsulfonylfluoride (PMSF) were obtained from Sigma-Aldrich (St. Louis, MA, USA).

Genomic analysis of Thermoplasma acidophilum genome

The genome of *Thermoplasma acidophilum DSM1728* (RefSeq NC_002578, GenBank AL139299) was analyzed using the web interface at the National Center for Biotechnology Information (http://www.ncbi.nlm.nih.gov) for putative thioredoxin reductase (TrxR) and thioredoxin (Trx) open reading frames (ORFs). An ORF encoding a 319 amino acid protein, Ta0984, and an ORF encoding for a 113 amino acid protein, Ta0866, were identified by

sequence homology to known TrxRs and Trxs using PSI-BLAST (18). Protein sequences were aligned using the program ClustalW (19) and the output was rendered using the web interface ESPript 2.2 (20) (Figure S1 and S2).

Cloning of taTrxR and taTrx

The *ta*TrxR and *ta*Trx genes were amplified by the polymerase chain reaction (PCR) using genomic DNA from a cell suspension and the primers 5′- A TGC CAT ATG GCA TAT GGA ATT TAA CCT GCA TGC AGT A-3′ and 5′-TCA GCC AAG CTT CAT TTT TTG GAT ATA GAA TCA-3′ for *ta*TrxR and 5′ A TGC CAT ATG GCA TAT GAA GAA TTA TAT GGG CTG CG-3′ and 5′-TAG CGG CCG CTC AGA CGG AAT CGC AGG GA-3′ for *ta*Trx (restriction sites are underlined). PCR products were cloned into the expression vector pET28a using NdeI and HindIII restriction enzymes for *ta*TrxR and NdeI and NotI for *ta*Trx. The sequence of the pET28a-taTrxR and pET28a-taTrx cDNA was confirmed at the MIT Biopolymers Sequencing Facility (Figures S3 and S4). After confirmation of the correct sequences, the resulting constructs were transformed into Rosetta™ (DE3)pLysS cells for facile protein expression.

Purification of recombinant taTrxR and taTrx

Rosetta™ (DE3)pLysS transformed with either pET28ataTrxR or pET28ataTrx constructs were used to inoculate TB media supplemented with 20 μg ml^{-1} kanamycin and 34 μg ml^{-1} chloroamphenicol. The culture was grown at 37°C to an OD_{600} of 0.8 and induced with 0.8 mM isopropylthio-ß-D-galactoside (IPTG) for 4 hrs. The cells were harvested by centrifugation, resuspended in lysis buffer (10 mM TRIS-HCl pH 8.0, 150 mM NaCl, 10 mM imidazole, 1 mM PMSF), and disrupted by sonication using a Digital Sonifier 250 (Branson, CN, USA). Insoluble material was removed by ultracentrifugation at 40,000 x g using a Beckman Avanti J-25 centrifuge (Beckman, PA, CA, USA). The supernatant was subjected to heating at 70°C for 45 min, and then centrifuged at 40,000 x g. The clarified supernatant was loaded onto a Ni-NTA column, washed with high salt buffer, and eluted with buffer containing 10 mM TRIS-HCl pH 8.0, 150 mM NaCl, 200 mM imidazole. Eluted fractions were analyzed by an SDS-PAGE 4-20% gel and those fractions containing proteins with comparable size to *ta*TrxR or *ta*Trx were concentrated using an Amicon (Millipore, MA, USA) stirred ultrafiltration cell.

The eluted protein was dialyzed overnight in 20 mM HEPES, pH 7.5, 20 mM NaCl, 0.5 mM EDTA, 1 mM 1,4-dithio-DL-threitol (DTT) with thrombin (0.05 unit ml^{-1}) to remove the N-terminal poly-His-tag. The digested protein fraction was loaded onto an SEC-30 high-prep size exclusion column from Amersham Biosciences (Piscataway, NJ, USA), which was pre-equilibrated with storage buffer (10 mM HEPES, pH 7.0, 20 mM NaCl). Fractions containing protein of either MW ~34 kDa (*ta*TrxR) or MW ~13 kDa (*ta*Trx) were concentrated using Centriprep YM-3 filter from Amicon (Millipore, Bedford, MA, USA). Protein purity was analyzed by SDS/PAGE 4-20% gel (Figure S5) and protein concentration was determined from the theoretical extinction coefficient at 280 nm (23,040 M^{-1} cm^{-1} for *ta*TrxR and 16,500 M^{-1}cm^{-1} for *ta*Trx) (ProtParam, ExPaSy web server). A Cary 300 spectrophotometer (Varian, CA, USA) was used to analyze the purified *ta*TrxR for flavin incorporation.

Temperature stability of NADPH and NADH

NADPH (0.22 μM) and NADH (0.26 μM) were analyzed for temperature dependent degradation in 50 mM TRIS-HCl, pH 7.5, 150 mM NaCl (Figure S6). Initial UV / visible spectra were collected at 20° C from 800 nm to 240 nm. The temperature was increased to 80° C and the reaction was allowed to equilibrate for 5 min before full spectra were collected. The reaction was cooled to 20° C and then another full spectrum was collected. To measure time dependent degradation, NADPH or NADH was heated to the desired temperature (20° C, 60°

C, and 80° C) and a reading was collected at 340 nm in 5 min increments for 45 min. Degradation of NADPH or NADH was inferred from the decrease in absorbance at 340 nm normalized to 100 % of the absorbance for the sample at time zero. Experiments were performed in triplicate.

Activity of taTrx measured by insulin and DTT assays

Purified *ta*Trx was assayed for disulfide reductase activity by the insulin reduction method (21). The standard assay mixture contained 1.25 mM bovine insulin, 100 mM potassium phosphate, pH 7.0, 2 mM EDTA and *ta*Trx (43 μM, 66 μM, or 70 μM). The reaction was initiated by the addition of 1 mM DTT. An increase in absorbance at 650 nm was monitored at 25 °C.

Purified oxidized *ta*Trx was also assayed for its ability to be reduced by *ec*TrxR using the DTNB method (22). Briefly, this colorimetric assay measures the Trx dependant reduction of DTNB to 5-thio-2-nitrobenzoic acid (TNB), which absorbs strongly at 405-414 nm, using TrxR and NADPH as electron donors. The reaction was performed using 3.8 μM *ec*TrxR, in 50 mM TRIS-HCl, pH 8.0, 2 mM EDTA, 0.5 mM NADPH, and 0.6 mM DTNB. Each assay was initiated by the addition of *ta*Trx (5 – 60 μM) to reaction mixture and the conversion of DTNB to TNB was monitored by the increase in absorbance at 412 nm.

Titration of taTrxR and ecTrxR with NADPH and NADH

*ta*TrxR (43.3 μM) was titrated with NADPH or with NADH (0.5 to 5.0 mole NAD(P)H / mole FAD) under anaerobic conditions at 59° C in 50 mM TRIS, pH 7.5, 150 mM NaCl. Spectra were collected from 800 nm to 240 nm to monitor the reduction of the enzyme bound flavin by NADPH or NADH. *ec*TrxR (40.5 μM) was titrated with NADPH or with NADH (0.5 to 5.0 mol NADPH or NADH / mol FAD) under anaerobic conditions at 25 °C in 50 mM TRIS, pH 7.5, 150 mM NaCl. Spectra for NADPH reduction of *ec*TrxR were recorded as described above, and were corrected for dilution. The reduction of bound FAD was monitored by observing the change in absorbance at 457 nm over 45 minutes. *ta*TrxR (43.3 μM) and *ec*TrxR (40.5 μM) were titrated with 2.5 mM NADPH or NADH for 45 minutes. For *ta*TrxR, spectra were collected every minute and for *ec*TrxR spectra were collected every 0.1 minute for initial 5 minutes and then every 5 minutes thereafter.

Ability of taTrxR to reduce taTrx

To verify that the reduced *ta*TrxR was capable of passing electrons to *ta*Trx, the xanthine/xanthine oxidase reduction system, described by Massey and co-workers, was used (23). After complete reduction of a sample of *ta*TrxR, the re-oxidation of *ta*TrxR (4 μM) was monitored spectroscopically in the visible region following the addition of *ta*Trx or *ec*Trx (8 μM). The *ta*TrxR reduction system was as follows: in a 1 cm path length cuvette stirred continuously and held at 25° C in an MBraun Labmaster glove box, a solution of 100mM phosphate buffer (pH 7.5) with 1 μM benzyl viologen, 250 μM xanthine and 4 μM *ta*TrxR, an aliquot of xanthine oxidase was added to a final concentration of ~ 0.25 nM, to initiate the reaction. This solution was monitored in the visible region of the spectrum, using an SI Photonics spectrophotometer contained within the glovebox, over the course of 1.5 hours, upon which complete reduction of the *ta*TrxR was achieved. Oxidized Trx was then added to a final concentration of 8 μM, and the spectral features were monitored.

Analysis of T. acidophilum genome for alternative redox regulation pathways

To investigate if *T. acidophilum* uses alternative characterized reduction pathways, the *T. acidophilum* genome was mined for known pathways by using NCBI BLAST (18) to compare known proteins involved in the formation of glutathione or of coenzyme F420 to the ORFs of

T. acidophilum. Pathway members were identified using ExPASy PATHWAY service (http://ca.expasy.org/cgi-bin/lists?pathway.txt).

Crystallization and data collection

*ta*TrxR was crystallized by incubating 2.0 μL of protein solution (65 mg mL^{-1} *ta*TrxR in 10 mM HEPES, pH 7.5 and 20 mM NaCl) and 2.0 μL of precipitant solution (0.28 M $MgCl_2$, 0.1 M Bis-Tris, pH 5.5, 25% (w/v) PEG 3350) in a sitting drop at room temperature. Crystals had rhombohedral geometry, and their bright yellow color confirmed the incorporation of flavin adenine dinucleotide (FAD) by the enzyme. Crystals appeared cubic and grew to approximately 100 μM per side in 3 to 4 days. These crystals were soaked for 30 seconds in a cryo-protectant solution of 0.28 M $MgCl_2$, 0.1 M Bis-Tris, pH 5.5, 25% (w/v) PEG 3350, 25% PEG 400, before cryo-cooling in liquid nitrogen.

All diffraction data were collected at 100 K at the Advanced Light Source (Berkeley, CA), beam line 5.0.2. Data were processed and scaled using DENZO and SCALEPACK from the HKL (24) program suite (See Table 1). The crystals belong to the I23 (I-centered cubic) space group ($a = b = c = 165.95$ Å), with one homodimer per asymmetric unit.

Molecular replacement solution and refinement

The crystal structure of the thioredoxin reductase was solved by the method of molecular replacement. Initial phases were obtained from a full length poly-alanine model of thioredoxin reductase from *Escherichia coli* (PDB code 1TDE) (25). The solution was found using PHASER (26) with two search models consisting of the flavin binding domain and the NADPH-binding domain of the *E. coli* structure, utilizing data from a resolution range of 4.0 – 12.0 Å. PHASER was first used to find a solution for the FAD-binding domain of *ta*TrxR (residues 1 – 126 and 250 – 319). This solution was fixed and a second round of molecular replacement was performed to find the NADPH-binding domain (residues 127 – 249).

Refinement was carried out in CNS (27) with rigid body refinement followed by simulated annealing. Manual fitting of amino acid residues was done using XFIT (28). Subsequent rounds of refinement included simulated annealing, energy minimization, and B-factor refinement without sigma cutoff. Topology and parameter files for the FAD moiety were obtained from HIC-UP (29) (PDB code 1N1P). Water molecules were added with CNS and were manually checked against $2F_o$-F_c and F_o-F_c electron density maps. A composite omit map was prepared in CNS and used to confirm the assignment of model atoms. The final model contains a biologically relevant dimer in the asymmetric unit, which consists of residues 14-319 for molecule ‘A’ of 319 and residues 13-319 of 319 for molecule ‘B’, one flavin molecule per monomer and 114 water molecules.

RESULTS

Cloning, purification, and characterization of taTrxR and taTrx

Using the *T. acidophilum* genome database, we identified two ORFs (Accession no. Ta0984 and Ta0866): one encoding a putative thioredoxin reductase and the other one encoding a thioredoxin homologue. The Ta0984 gene encodes a protein of 319 amino acids with a predicted molecular mass of 34116 Da (Figure S3). The deduced amino acid sequence contains 28% identity (48% similar) to the *ec*TrxR (Figure S1). The Ta0866 gene encodes a 133 amino acid protein (Figure S4) with a CxxC disulfide-reducing motif and displays 34% identity (58% similarity) to *ec*Trx(Figure S2). These ORFs have been amplified by PCR, cloned, sequenced, and compared to the sequence in the *T. acidophilum* genome database.

The purified *ta*TrxR yields visible absorption spectra typical for flavoproteins with absorbance maxima at 380 and 460 nm. Freshly purified protein has an A_{280} / A_{460} ratio of between 7.5 and 8.0, in agreement with the full incorporation of FAD as previously observed for *ec*TrxR (30). Expression and subsequent purification yields ~18.5 mg from a 1 liter culture. The molecular mass of the protein is estimated to be approximately 34 kDa by SDS-PAGE (Figure S5a). This molecular mass is in agreement with values predicted by the gene analysis. The native molecular mass is determined to be about 70 kDa by gel-filtration using a Sephacryl SEC-75 HR 16/60 column. These results suggest that the native state of *ta*TrxR is a homodimer, similar to *ec*TrxR (31). Expression of *ta*Trx yields a protein of 13.2 kDa as analyzed by SDS PAGE (Figure S5b). Subsequent gel-filtration using a Sephacryl SEC-30 HR 16/60 column reveals a native molecular mass of ~13 kDa, suggesting that the *ta*Trx is a monomer in its native state.

Lack of activity of taTrxR with NADPH or NADH

All previously characterized TrxRs are reduced by NADPH (Reviewed in (2,32,33)). For *ec*TrxR, reaction of NADPH with the FAD cofactor occurs rapidly (2,000 turnovers FAD^{-1} min^{-1}) with a K_m for NADPH of 1.2 μM (34). While there is no measurement of K_m for NADH with *ec*TrxR, it has been estimated to be 400 fold higher than that of NADPH (31). Therefore, it is surprising that titration of *ta*TrxR with concentrations of up to 5 fold molar excess NADPH does not reduce its FAD cofactor to any appreciable extent, showing no significant spectral change in the visible part of the spectra (Figure 2A). For comparison, titration of *ec*TrxR with NADPH results in a rapid reduction of the bound FAD, decreasing the absorbance at 460 nm (Figure 2C). Titration of *ta*TrxR with NADH shows minimal reduction of FAD as indicated by the small change in the shoulder at 460 nm (Figure 2B). Although NADPH is the preferred substrate for *ec*TrxR, NADH does reduce the flavin to some extent in this protein (Figure 2D). The reduction is, in fact, greater than that observed for *ta*TrxR. Compared to the rapid reduction of *ec*TrxR by NADPH (turnover rate is 2,000 FAD^{-1} min^{-1}) (34), the changes observed for *ta*TrxR appear too slow and too small to be physiologically relevant (Figure 2E). The inability of NADPH or NADH to rapidly reduce *ta*TrxR is not due to instability of these components at 59 °C, the physiological temperature of *T. acidophilum*. Analysis of the time-dependent degradation of NADPH and NADH at 59 °C shows that there is negligible degradation at 5 min under assay conditions, not enough to explain this lack of activity (Figure S6). At the higher temperature of 80°C, degradation is increased, but even then less than 10% of NADPH or NADH is degraded during the first five minutes of the assay, and only 30% is degraded by 45 minutes (Figure S6).

Disulfide reductase activity of taTrx

The lack of measurable activity between *ta*TrxR and NADPH prevented the use of a coupled assay for *ta*Trx activity, requiring us to turn to other methods to characterize the *ta*Trx. The reduction of insulin disulfides can be monitored by following the increase in turbidity at 650 nm due to the precipitation of the free B-chain (21). The recombinant *ta*Trx reduced insulin in a protein concentration-dependent manner (Figure S7). To investigate whether *ta*Trx is able be reduced by *ec*TrxR we performed the DTNB assay using NADPH, *ec*TrxR, and *ta*Trx. *ta*Trx is reduced by *ec*TrxR, with an estimate of the apparent K_m of 14.4 (±7.0) μM for the *ec*TrxR (Figure S8). This K_m value is higher than for the *ec*TrxR / *ec*Trx system (K_m of 2.8 μM) (31), which is not surprising in that the two proteins (*ec*TrxR and *ta*Trx) did not evolve to interact. These experiments confirm that the *ta*Trx is a thioredoxin-like protein capable of performing disulfide exchange.

Thioredoxin reductase activity of taTrxR

To verify that *ta*TrxR can catalyze a disulfide exchange with *ta*Trx, we pre-reduced *ta*TrxR using a modified xanthine / xanthine oxidase system (see methods) at 25° C; after complete reduction of the *ta*TrxR flavin, the reduced enzyme was treated with oxidized *ta*Trx. Upon the introduction of two equivalents of *ta*Trx, the *ta*TrxR was rapidly oxidized, achieving complete re-oxidation of the FAD within one min (Figure 3). This experiment indicates that *ta*TrxR is a biologically relevant TrxR, which does not use NADPH as a reductant.

Overall Structure

The structure of *ta*TrxR was solved to 2.35 Å resolution with the physiological dimer in the asymmetric unit and an R and R_{free} of 22.6% and 26.8%, respectively (See Table 1 for statistics). Each *ta*TrxR monomer consists of an FAD-binding domain (residues 14-125 and 251-319) and an "NADPH binding domain" (residues 126-250) (Figure 4A). Each domain of *ta*TrxR is quite similar to the equivalent domain of *ec*TrxR, with an r.m.s.d. of 1.23 Å for the 166 Cα of the FAD-binding domain, and an r.m.s.d of 1.17 Å for 121 Cα of the "NADPH-binding domains" (Figure 4B and 4C). The *ta*TrxR structure has one FAD molecule bound in a similar conformation as the *ec*TrxR structure (Figure S9), and with similar protein-FAD interactions (Figure S10).

*ec*TrxR is known to undergo a large conformational change during catalysis, rotating between a "flavin oxidizing" form (FO) and a "flavin reducing" form (FR) (25,35,36). In the FR form, the FAD domain is positioned such that NADPH can reduce the FAD by hydride transfer (Figure 4A). In the FO form, the FAD domain is positioned adjacent to the disulfide such that the $FADH_2$ can be oxidized by the disulfide. Structures of both conformations are available for the *E. coli* enzyme: the structure of wild type *ec*TrxR represents the FO state, and a structure of a complex between *ec*TrxR and *ec*Trxrepresents the FR state. Interestingly, while all other structures of uncomplexed TrxRs are in the FO state, the *ta*TrxR structure is of the FR form. The *ta*TrxR FR conformation is very similar to that of *ec*TrxR in the FR state with an r.m.s.d. of 1.30 Å for chain A and 1.73 Å for chain B when all the Cα atoms are superimposed. As with the *ec*TrxR FR structure, the *ta*TrxR FAD domain is positioned near the putative NADPH binding site, and away from the catalytic cysteines (Cys145 and Cys148), which are oxidized with an S-S distance of 2.04 Å. A discussion of the conformational dynamics of TrxRs is available in the accompanying paper.

Major Differences in the Domain that Typically Binds NADPH

Structural superposition of the "NADPH binding domains" from *ec*TrxR and *ta*TrxR reveal that the backbone of residues 184 - 191 of the *ta*TrxR structure is constrained into a slightly different conformation than is found in *ec*TrxR. This different loop conformation appears to result from the presence of a proline (P188) in the *ta*TrxR sequence (Figure 5C), and not the presence or absence of nucleotide in the structure (Figure S12). This variation in loop conformation is subtle and is unlikely to explain the lack of affinity of NADPH for the *ta* enzyme. In contrast, while the "NADPH-binding domains" for *ta*TrxR and *ec*TrxR display an overall similar fold, close examination reveals several highly conserved residues in all bacterial TrxRs that are not conserved in the *ta*TrxR sequence. The *ec*TrxR structure, which was co-crystallized with $NADP^+$, shows that the NADPH 2′ phosphate is surrounded by a histidine (H175) and three arginines (R176, R177, and R181) creating a positively charged pocket that complements the negatively charged phosphate (Figures 5A, 6A, and S11A). The lower activity (400-fold) for NADH compared to NADPH (31) is presumably due to the loss of interactions between the cofactor and residues that form this positively charged pocket (Figure 6C). In *ta*TrxR, none of the residues that form this pocket are conserved. The classic NADPH binding motif 'VxxxHRRDxxRA' is replaced with 'VxxxEYMPxxMC' in *ta*TrxR (Figure 5D). *ec*TrxR's histidine 175, which points directly toward the 2′ phosphate of the NADPH, is

substituted with a glutamic acid (E185) in *ta*TrxR, and the three arginine residues (R176, R177, and R181) are replaced by a tyrosine (Y186) and two methionines (M187 and M191) (Figures 5B and 5C). These substitutions dramatically change the electrostatics of this protein surface (Figures 6 and S11). In a model of NADH bound to *ta*TrxR, an unfavorable interaction between E185 and the 2′ phosphate of NADPH is relieved (Figure 6D), but neither NADPH nor NADH would be expected to bind with any kind of reasonable affinity, consistent with the lack of rapid reduction of FAD by these molecules. Analysis of all known bacterial and archaeal genomes shows that only one other organism, the close cousin to *T. acidophilum*, *Thermoplasma volcanicum*, contains an identical 'VxxxEYMPxxMC' sequence. All others use a variant of the Arg-rich 'VxxxHRRDxxRA' motif.

DISCUSSION

The protein derived from Ta0984 is a thioredoxin reductase. Our structural and biochemical studies reveal a protein with an FAD cofactor and an overall similar fold to the *ec*TrxR. However, unlike all other characterized TrxRs, *ta*TrxR is not reduced by NADPH. This lack of reactivity is unlikely to be due to redox potential differences between TrxRs (See accompanying paper). The redox potential of *ta*TrxR is within 35 mV of *ec*TrxR (−305 vs. −270 mV) (37), and when reduced with a xanthine / xanthine oxidase system, *ta*TrxR is able to react stoichiometrically with *ta*Trx.

Examination of the *ta*TrxR structure suggests that the lack of activity with NADPH is due to amino acid substitutions as compared to the *E. coli* enzyme. The "NADPH-binding site" of *ta*TrxR does not appear to be designed to bind NADPH, with neutral and negatively charged amino acids replacing the canonical Arg-rich motif. The "NADPH-binding site" is also structurally constrained by P188. Sequence analysis shows that only one other organism, the closely related *Thermoplasma volcanicum*, shares *ta*TrxR's unusual sequence.

The lack of a NADPH-dependent TrxR / Trx reduction system in *T. acidophilum* led us to investigate whether this organism might rely heavily on GSSGR / Grx systems instead of on thioredoxins. Analysis of the *T. acidophilum* genome, however, revealed no GSSGR / Grx system, nor enzymes for the biosynthesis of glutaredoxin (38). Our extensive data mining and sequence alignments have not produced any near or distantly related GSSGR / Grx proteins from this organism.

We also considered whether *T. acidophilum* uses NADH or NADPH in other cellular processes. Our genomic analysis reveals a putative NAD kinase, the enzyme responsible for the conversion of NAD to NADP, and several putative NADH and NADPH utilizing enzymes, which suggests that *T. acidophilium* does use these cofactors. To date, there are only a few characterized enzymes in *T. acidophilum* that use NADH (aldohexose dehydrogenase) (39) or NADPH (glyderaldehyde dehydrogenase) (40) or both NADH and NADPH as substrates (41). However, the use of NADPH or NADH by any *T. acidophilum* enzyme, in addition to the presence of the NAD kinase gene, indicates that availability of these cofactors is not the reason for the observed variation in the TrxR protein.

The above data challenges the paradigm shown in Figure 1A. Our data blocks the arrow to the left, and the lack of GSSGR / Grx blocks the arrow to the right. Given this, we revisited the *T. acidophilum* genome to search again for other putative TrxR sequences and found none. Unless there is a TrxR with a very different sequence, we have cloned the only one in *T. acidophilum*.

If NADPH does not reduce this *ta*TrxR, and this TrxR is the only TrxR in *T. acidophilum*, and there are no obvious GSSGR / Grx candidates, there must be some small molecule that can provide reducing equivalents or the cytoplasmic environment would quickly oxidize and the

organism would expire. One such molecule, coenzyme F420, has been shown to be a physiological reductant in methane reducing thermophilic organisms (Reviewed in (42-44)). However, genomic analysis of *T. acidophilum* does not reveal any of the enzymes involved in the biosynthesis of F420. The lack of molecular pathways for the biosynthesis of coenzyme F420, along with the lack of other F420-dependent enzymes in *T. acidophilum*, seems to indicate that coenzyme F420 is not a reductant of *ta*TrxR. Of course, we cannot rule out the possibility that F420 is generated by a different set of enzymes in this organism.

Conclusions

To date, there is no well characterized example of an organism that uses a reductant other than NADPH to maintain its intracellular redox environment. Here we present evidence that one organism, *T. acidophilum*, which does not contain a Grx system, uses an alternative method to reduce the bound FAD of the TrxR system. This work lays the foundation for a biochemical search for the molecular redox partners of *T. acidophilum* TrxR.

Supplementary Material

Refer to Web version on PubMed Central for supplementary material.

Acknowledgments

The authors would like to thank Dr. Scott Mulrooney and Prof. Charles Williams, Jr. for the generous donation of the *ec*TrxR over-expression system. Portions of this research were carried out at the Stanford Synchrotron Radiation Laboratory, a national user facility operated by Stanford University on behalf of the U.S. Department of Energy, Office of Basic Energy Sciences. The SSRL Structural Molecular Biology Program is supported by the Department of Energy, Office of Biological and Environmental Research, and by the National Institutes of Health, National Center for Research Resources, Biomedical Technology Program, and the National Institute of General Medical Sciences.

Abbreviations

Trx	thioredoxin
TrxR	thioredoxin reductase
Grx	glutaredoxin
GDH	glutathione
GSSGR	glutathione reductase
RNR	ribonucleotide reductase
ORF	open reading frame
TRIS-HCl	tris(hydroxymethyl)-aminomethane hydrochloride
PMSF	phenyl methyl sulfonyl fluoride
PCR	polymerase chain reaction
DTT	1,4-dithio-DL-theritol
HEPES	N-2-hydroxyethyl-piperazine-N'-2-ethanesulfonic acid
Ec	Escherichia coli
EDTA	ethylenediaminetetraacetic acid
FAD	flavin adenine dinucleotide
$FADH_2$	flavin adenine dinucleotide, reduced form
FO	flavin oxidizing conformation

FR	flavin reducing conformation
NADH	nicotinamide adenine dinucleotide, reduced form
NADPH	nicotinamide adenine dinucleotide phosphate, reduced form
SafO	safranine O
Ta	Thermoplasma acidophilum
XO	xanthine oxidase

REFERENCES

1. Jaeger T, Flohe L. The thiol-based redox networks of pathogens: unexploited targets in the search for new drugs. Biofactors 2006;27(14):109–120. [PubMed: 17012768]
2. Arner ES, Holmgren A. Physiological functions of thioredoxin and thioredoxin reductase. Eur J Biochem 2000;267(20):6102–6109. [PubMed: 11012661]
3. Masutani H, Ueda S, Yodoi J. The thioredoxin system in retroviral infection and apoptosis. Cell Death Differ 2005;12(Suppl 1):991–998. [PubMed: 15818395]
4. Gromer S, Urig S, Becker K. The thioredoxin system--from science to clinic. Med Res Rev 2004;24 (1):40–89. [PubMed: 14595672]
5. Mustacich D, Powis G. Thioredoxin reductase. Biochem J 2000;346(Pt 1):1–8. [PubMed: 10657232]
6. Stroher E, Dietz KJ. Concepts and approaches towards understanding the cellular redox proteome. Plant Biol (Stuttg) 2006;8(4):407–418. [PubMed: 16906481]
7. Toledano MB, Kumar C, Le Moan N, Spector D, Tacnet F. The system biology of thiol redox system in Escherichia coli and yeast: differential functions in oxidative stress, iron metabolism and DNA synthesis. FEBS Lett 2007;581(19):3598–3607. [PubMed: 17659286]
8. Herrick J, Sclavi B. Ribonucleotide reductase and the regulation of DNA replication: an old story and an ancient heritage. Mol Microbiol 2007;63(1):22–34. [PubMed: 17229208]
9. Nordlund P, Reichard P. Ribonucleotide reductases. Annu Rev Biochem 2006;75:681–706. [PubMed: 16756507]
10. Shao J, Zhou B, Chu B, Yen Y. Ribonucleotide reductase inhibitors and future drug design. Curr Cancer Drug Targets 2006;6(5):409–431. [PubMed: 16918309]
11. Hashemy SI, Ungerstedt JS, Zahedi Avval F, Holmgren A. Motexafin gadolinium, a tumor-selective drug targeting thioredoxin reductase and ribonucleotide reductase. J Biol Chem 2006;281(16): 10691–10697. [PubMed: 16481328]
12. Urig S, Becker K. On the potential of thioredoxin reductase inhibitors for cancer therapy. Semin Cancer Biol 2006;16(6):452–465. [PubMed: 17056271]
13. Becker K, Gromer S, Schirmer RH, Muller S. Thioredoxin reductase as a pathophysiological factor and drug target. Eur J Biochem 2000;267(20):6118–6125. [PubMed: 11012663]
14. Darland G, Brock TD, Samsonoff W, Conti SF. A thermophilic, acidophilic mycoplasma isolated from a coal refuse pile. Science 1970;170(965):1416–1418. [PubMed: 5481857]
15. Searcy DG. Thermoplasma acidophilum: intracellular pH and potassium concentration. Biochim Biophys Acta 1976;451(1):278–286. [PubMed: 12804]
16. Hsung JC, Haug A. Intracellular pH of Thermoplasma acidophila. Biochim Biophys Acta 1975;389 (3):477–482. [PubMed: 236035]
17. Ruepp A, Graml W, Santos-Martinez ML, Koretke KK, Volker C, Mewes HW, Frishman D, Stocker S, Lupas AN, Baumeister W. The genome sequence of the thermoacidophilic scavenger Thermoplasma acidophilum. Nature 2000;407(6803):508–513. [PubMed: 11029001]
18. Altschul SF, Madden TL, Schaffer AA, Zhang J, Zhang Z, Miller W, Lipman DJ. Gapped BLAST and PSI-BLAST: a new generation of protein database search programs. Nucleic Acids Res 1997;25 (17):3389–3402. [PubMed: 9254694]
19. Higgins D, Gibson T.Thompson JD, Higgins DG, Gibson TJ. CLUSTAL W: improving the sensitivity of progressivemultiple sequence alignment through sequence weighting,position-specific gap

penalties and weight matrix choice. Nucleic Acids Res 1994;(22):4673–4680. T. J. [PubMed: 7984417]

20. Gouet P, Courcelle E, Stuart DI, Metoz F. ESPript: analysis of multiple sequence alignments in PostScript. Bioinformatics 1999;15(4):305–308. [PubMed: 10320398]
21. Holmgren A. Thioredoxin catalyzes the reduction of insulin disulfides by dithiothreitol and dihydrolipoamide. J Biol Chem 1979;254(19):9627–9632. [PubMed: 385588]
22. Arner ES, Zhong L, Holmgren A. Preparation and assay of mammalian thioredoxin and thioredoxin reductase. Methods Enzymol 1999;300:226–239. [PubMed: 9919525]
23. Massey V, Brumby PE, Komai H. Studies on milk xanthine oxidase. Some spectral and kinetic properties. J Biol Chem 1969;244(7):1682–1691. [PubMed: 5813728]
24. Otwinowski Z, Minor W. Processing of X-ray Diffraction Data Collected in Oscillation Mode. Methods Enzymol 1997;276:307–326.
25. Waksman G, Krishna TS, Williams CH Jr. Kuriyan J. Crystal structure of Escherichia coli thioredoxin reductase refined at 2 A resolution. Implications for a large conformational change during catalysis. J Mol Biol 1994;236(3):800–816. [PubMed: 8114095]
26. McCoy AJ, Grosse-Kunstleve RW, Storoni LC, Read RJ. Likelihood-enhanced fast translation functions. Acta Crystallogr D Biol Crystallogr 2005;61(Pt 4):458–464. [PubMed: 15805601]
27. Brunger AT, Adams PD, Clore GM, DeLano WL, Gros P, Grosse-Kunstleve RW, Jiang JS, Kuszewski J, Nilges M, Pannu NS, Read RJ, Rice LM, Simonson T, Warren GL. Crystallography & NMR system: A new software suite for macromolecular structure determination. Acta Crystallogr D Biol Crystallogr 1998;54(Pt 5):905–921. [PubMed: 9757107]
28. McRee DE. XtalView/Xfit--A versatile program for manipulating atomic coordinates and electron density. J Struct Biol 1999;125(23):156–165. [PubMed: 10222271]
29. Kleywegt GJ, Jones TA. Databases in protein crystallography. Acta Crystallogr D Biol Crystallogr 1998;54(Pt 6 Pt 1):1119–1131. [PubMed: 10089488]
30. Williams CH Jr. Zanetti G, Arscott LD, McAllister JK. Lipoamide dehydrogenase, glutathione reductase, thioredoxin reductase, and thioredoxin. J Biol Chem 1967;242(22):5226–5231. [PubMed: 4863745]
31. Thelander L. Thioredoxin reductase. Characterization of a homogenous preparation from Escherichia coli B. J Biol Chem 1967;242(5):852–859. [PubMed: 5335913]
32. Williams CH, Arscott LD, Muller S, Lennon BW, Ludwig ML, Wang PF, Veine DM, Becker K, Schirmer RH. Thioredoxin reductase two modes of catalysis have evolved. Eur J Biochem 2000;267 (20):6110–6117. [PubMed: 11012662]
33. Biaglow JE, Miller RA. The thioredoxin reductase/thioredoxin system: novel redox targets for cancer therapy. Cancer Biol Ther 2005;4(1):6–13. [PubMed: 15684606]
34. Williams, CH, Jr.. Flavin-Containing Dehydrogenases. In: Boyer, PD., editor. The Enzymes. Vol. Third Edition ed.. Vol. 1. Academic Press; New York: 1976. p. 89-173.
35. Lennon BW, Williams CH Jr. Ludwig ML. Crystal structure of reduced thioredoxin reductase from Escherichia coli: structural flexibility in the isoalloxazine ring of the flavin adenine dinucleotide cofactor. Protein Sci 1999;8(11):2366–2379. [PubMed: 10595539]
36. Wang PF, Veine DM, Ahn SH, Williams CH Jr. A stable mixed disulfide between thioredoxin reductase and its substrate, thioredoxin: preparation and characterization. Biochemistry 1996;35(15): 4812–4819. [PubMed: 8664271]
37. O'Donnell ME, Williams CH Jr. Proton stoichiometry in the reduction of the FAD and disulfide of Escherichia coli thioredoxin reductase. Evidence for a base at the active site. J Biol Chem 1983;258 (22):13795–13805. [PubMed: 6358211]
38. Copley SD, Dhillon JK. Lateral gene transfer and parallel evolution in the history of glutathione biosynthesis genes. Genome Biol 2002;3(5):1–16.
39. Reher M, Schonheit P. Glyceraldehyde dehydrogenases from the thermoacidophilic euryarchaeota Picrophilus torridus and Thermoplasma acidophilum, key enzymes of the non-phosphorylative Entner-Doudoroff pathway, constitute a novel enzyme family within the aldehyde dehydrogenase superfamily. FEBS Lett 2006;580(5):1198–1204. [PubMed: 16458304]

40. Nishiya Y, Tamura N, Tamura T. Analysis of bacterial glucose dehydrogenase homologs from thermoacidophilic archaeon Thermoplasma acidophilum: finding and characterization of aldohexose dehydrogenase. Biosci Biotechnol Biochem 2004;68(12):2451–2456. [PubMed: 15618614]

41. Smith LD, Budgen N, Bungard SJ, Danson MJ, Hough DW. Purification and characterization of glucose dehydrogenase from the thermoacidophilic archaebacterium Thermoplasma acidophilum. Biochem J 1989;261(3):973–977. [PubMed: 2803257]

42. Fischer M, Bacher A. Biosynthesis of flavocoenzymes. Nat Prod Rep 2005;22(3):324–350. [PubMed: 16010344]

43. Graupner M, Xu H, White RH. The pyrimidine nucleotide reductase step in riboflavin and F(420) biosynthesis in archaea proceeds by the eukaryotic route to riboflavin. J Bacteriol 2002;84(7):1952–1957. [PubMed: 11889103]

44. Mack M, Grill S. Riboflavin analogs and inhibitors of riboflavin biosynthesis. Appl Microbiol Biotechnol 2006;71(3):265–275. [PubMed: 16607521]

45. Baker NA, Sept D, Joseph S, Holst MJ, McCammon JA. Electrostatics of nanosystems: application to microtubules and the ribosome. Proc Natl Acad Sci U S A 2001;98(18):10037–10041. [PubMed: 11517324]

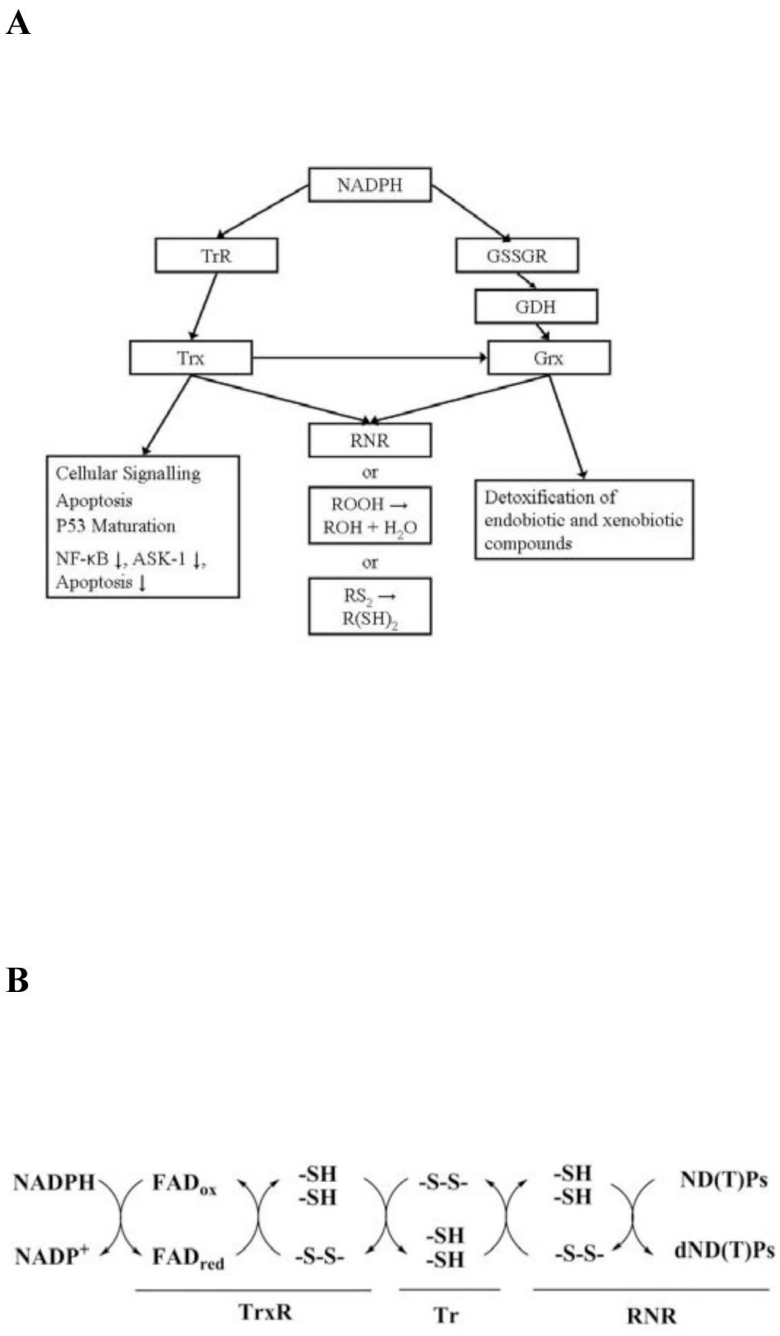

Figure 1.
NADPH participation in cellular redox regulation. (A) The NADPH-dependent redox regulatory pathways. (B) Mechanism of NADPH-dependent cellular reduction by the thioredoxin reductase system.

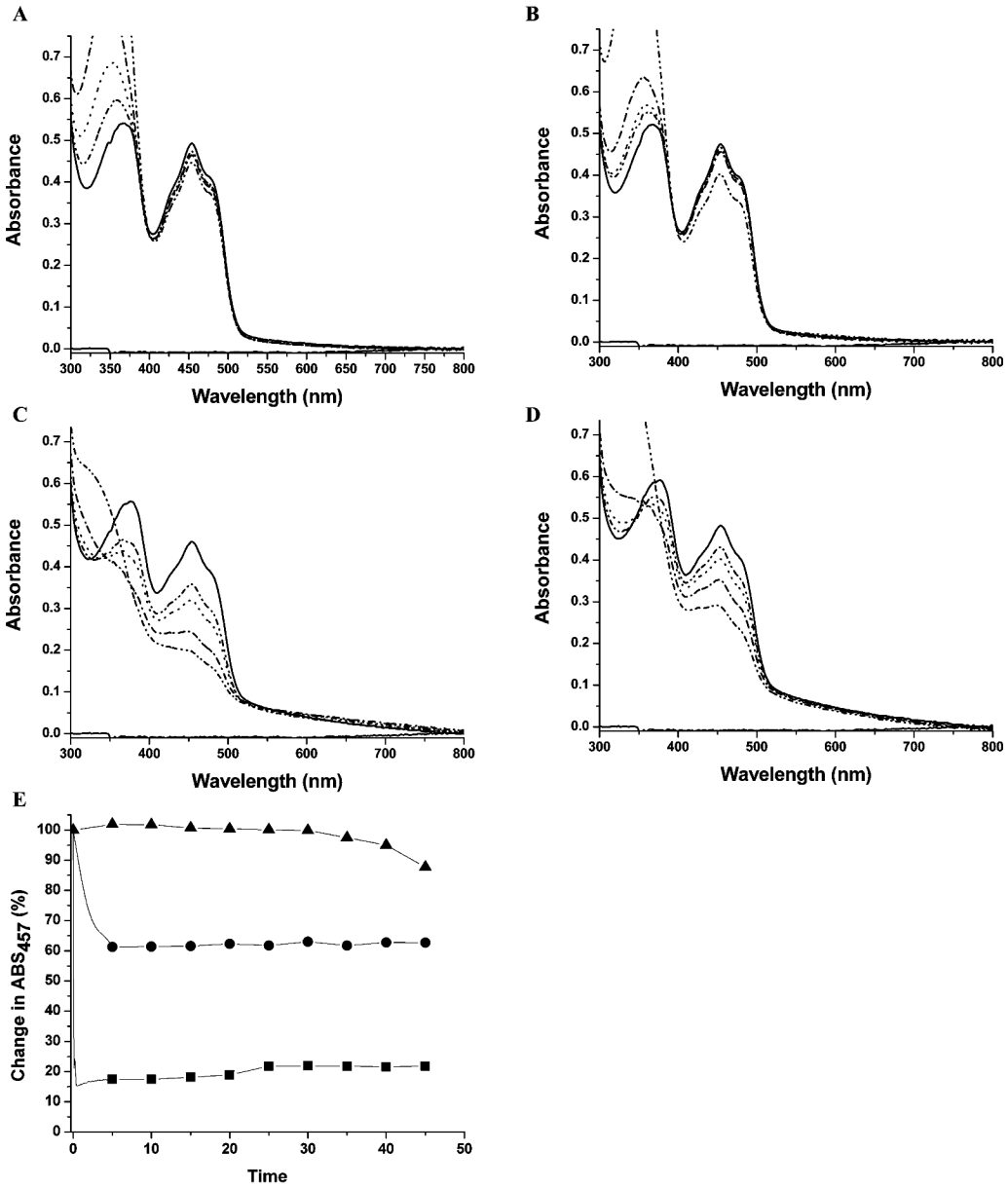

Figure 2.

Anaerobic titration of *ta*TrxR and *ec*TrxR with NADPH and NADH. (A) Visible spectra of *ta*TrxR (43.3 μM) titrated with NADPH at 59 °C. Solid line is without NADPH, dashed line is with 0.5 moles NADPH / mole FAD, dotted line is with 1.0 mole NADPH, dash dot line is with 2.0 mole NADPH, dash dot dot line is with 5 mole NADPH. (B) Visible spectra of *ta*TrxR titrated with NADH at 59 °C. (C) Visible spectra of *ec*TrxR (40.5 μM) titrated with NADPH at 25 °C. (D) Visible spectra of *ec*TrxR (40.5 μM) titrated with NADH at 25 °C. Spectra (B), (C), and (D) were recorded as in (A). (E) Time dependent reduction of *ta*TrxR and NADPH at 59 °C (closed triangles), *ta*TrxR and NADH at 59 °C (closed circles), and *ec*TrxR at 25 °C with NADPH (closed squares).

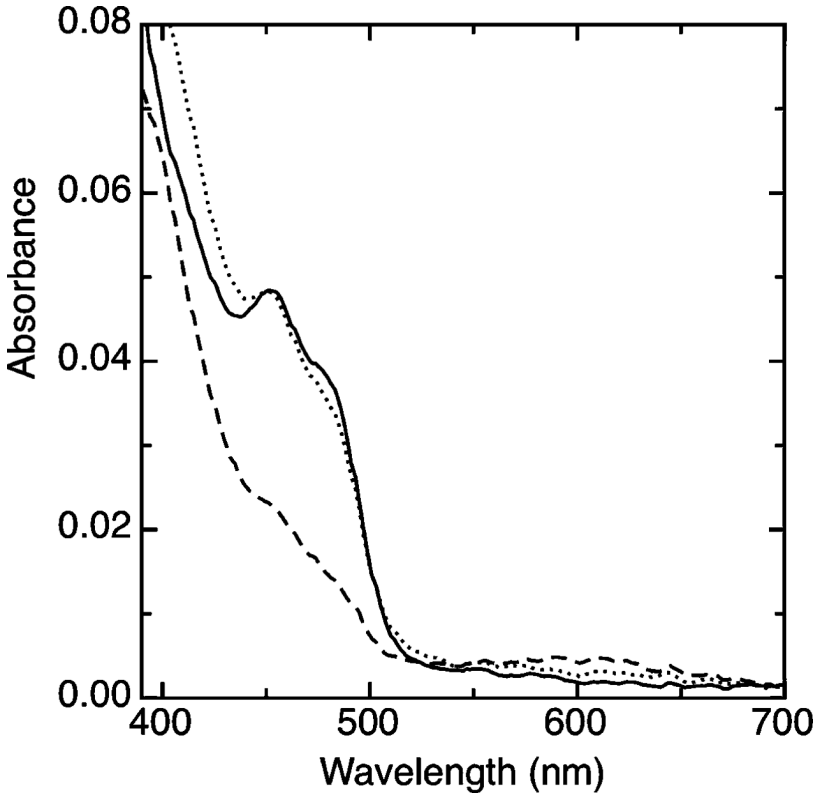

Figure 3.

Demonstration of *ta*TrxR/Trx reactivity. Reduction of oxidized *ta*TrxR (4 μM) was achieved by use of a modified xanthine/xanthine oxidase system, as described in the Materials and Methods section. Oxidized *ta*TrxR (solid line) was reduced with xanthine as the source of electrons, over the course of 90 minutes, in order to build up a stable reduced form of the enzyme (dashed line). Upon introduction of 2 equivalents of the *ta*Trx, the sample was completely reoxidized within 1 minute (dotted line).

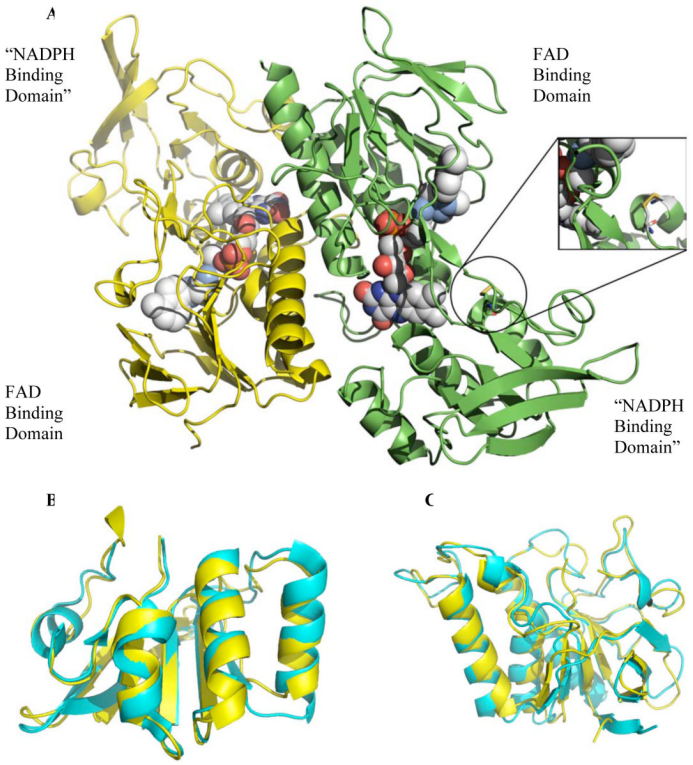

Figure 4.

Ribbon diagram structure of *ta*TrxR dimer. (A) Monomers of *ta*TrxR are colored by chain. The flavin molecule (1 per monomer) is represented as space filled spheres and colored by atom (C in light grey, N in blue, O in red, P in orange). Circle highlights C145/C148 disulfide. (B) Superposition of the *ta*TrxR NADPH binding domain with *ec*TrxR NADPH binding domain. (C) Superposition of the *ta*TrxR FAD binding domain in yellow with *ec*TrxR FAD binding domain in cyan.

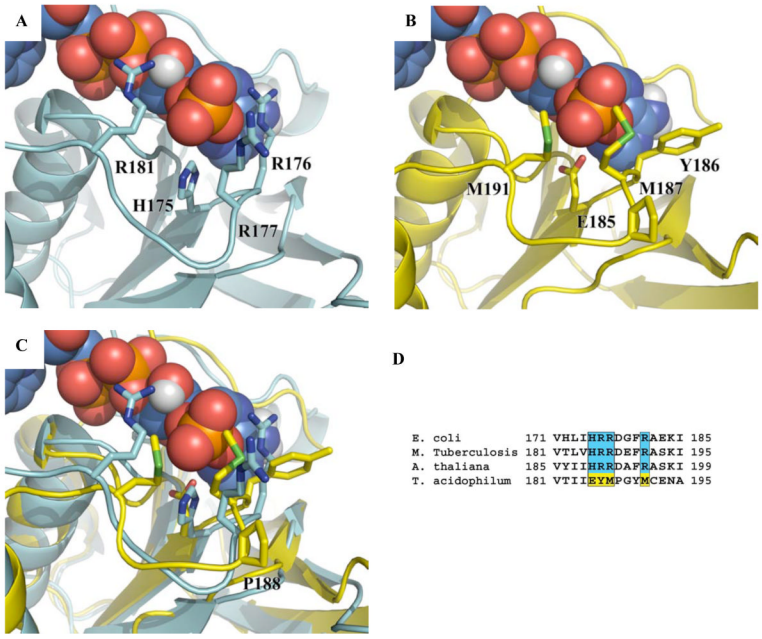

Figure 5.

Ribbon representation of the *ec*TrxR NADPH binding domain (cyan) (PDB code 1TDF) and *ta*TrxR "NADPH binding domain" (yellow). (A) *ec*TrxR with NADPH binding amino acids, H175, R176, R177, and R181, represented in stick form. (B) *ta*TrxR structure with corresponding structurally aligned amino acids, E185, Y186, M187 and M191 represented in stick form with modeled NADPH. (C) Superposition of *ec*TrxR and *ta*TrxR NADPH binding domains with NADPH from *ec*TrxR structure (D) Sequence alignment of the NADPH binding domain regions.

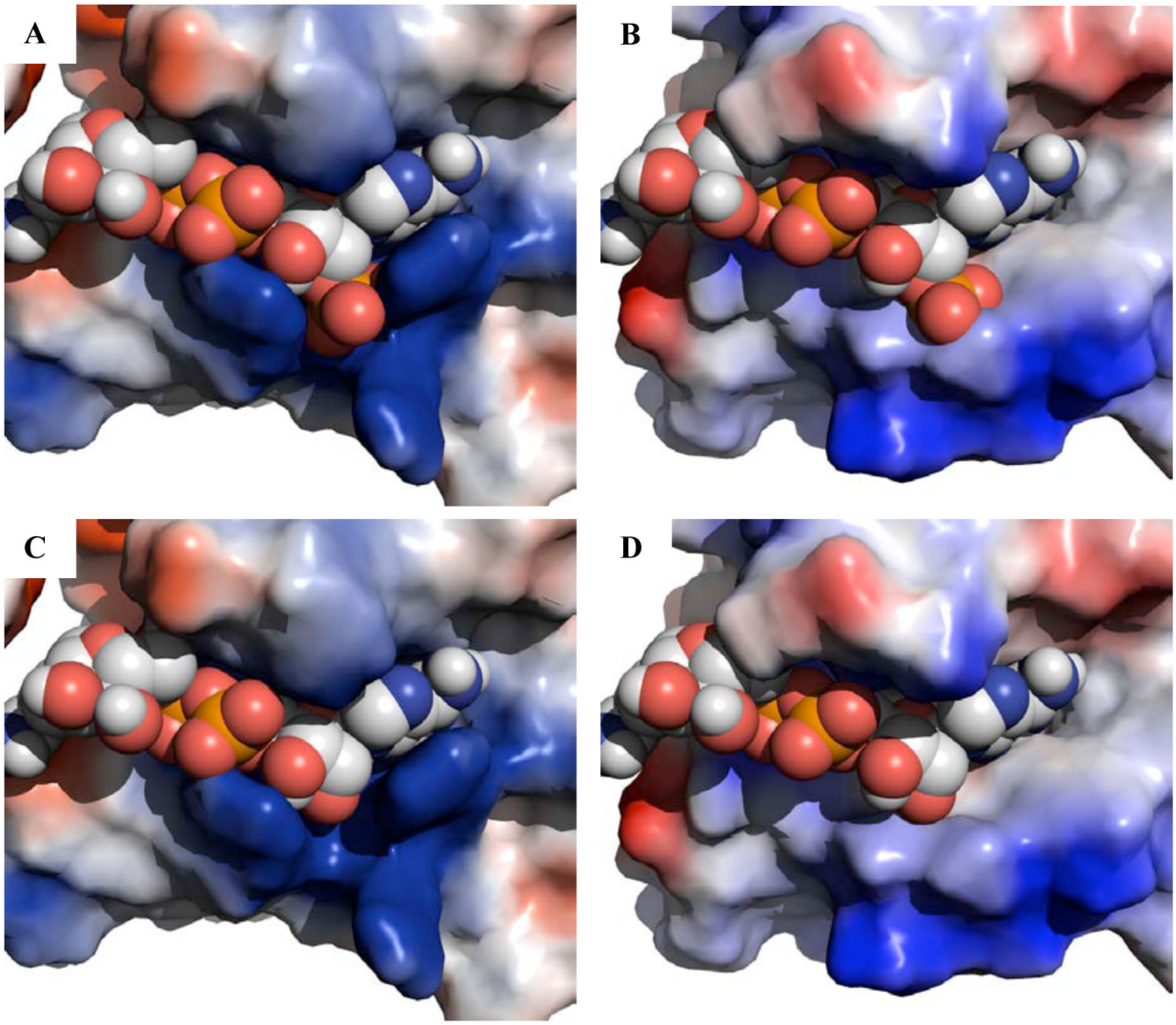

Figure 6.

Surface representation of NADPH binding pocket with blue representing basic residues, red acidic residues, and white neutral residues. (A) *ec*TrxR structure with NADPH bound. (B) *ta*TrxR structure with modeled NADPH. (C) *ec*TrxR structure with NADH modeled in the NADPH binding site. (D) *ta*TrxR structure with NADH modeled in the NADPH binding site. The orientations shown in Figure 6 are similar to those shown in Figure 5, with the panels in Figure 6 rotated slightly to the left so that the NAD(P)H adenine rings are more clearly visible. Surface calculations were made using the APBS module in Pymol (45).

Table 1

Data and refinement statistics for or *ta*TrxR structure

Dataset	**Native**
Wavelength (Å)	1.2710
Beamline	ALS 5.0.2
Space Group	I23
a=b=c (Å)	165.95
Resolution (Å)	50. - 2.35
R_{sym} (%)	6.9 (52.1)[a]
No. of Observations	434,549
Unique Observation	31,586
I/σI	32.9 (7.6)
Completeness (%)	99.9 (100.0)
Refinement Statistics	
Resolution Limits (Å)	50. - 2.35
# Unique Reflections	31,128
# Reflections - Test Set	1,809
R_{work} (%)[b]	22.5
R_{free} (%)[c]	26.0
Wilson B factor (Å)	68.3
B factor Chain A (Å)	55.4
B factor Chain B (Å)	62.1
B factor FAD 1 (Å)	49.2
B factor FAD 2 (Å)	59.4
B factor Waters (Å)	68.0
Solvent Content (%)	56.4
# protein atoms	2272 (2285)[d]
# water atoms	111
# non-protein atoms (FAD)	106
Bond length deviation (Å)	0.0073
Bond angle deviation (°)	1.2
Ramachandran Plot	
Residues in most favored regions (%)	93.6
Res in allowed region (%)	6.2
Res in disallowed region (%)	0.2

[a] Statistics for highest resolution shell (2.35 Å to 2.43 Å) are in parentheses

[b] $R_{work} = \Sigma||Fobs| - |Fcalc|| / \Sigma|Fobs|$

[c] R_{free} calculated using 5% of the total reflections, which were not used in refinement

[d] Number of atoms in chain A and chain B